

Characterization of Two Chloro-Substituted *m*-Benzyne Isomers: Effect of Substitution on Reaction Efficiencies and Products

Jason M. Price and Hilkka I. Kenttämäa*

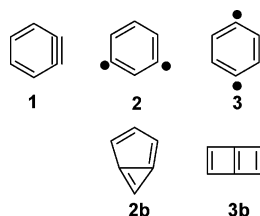
Department of Chemistry, Purdue University, West Lafayette, Indiana 47907-1393

Received: May 9, 2003

Two isomeric chloro-substituted *N*-phenylpyridinium-type *m*-benzyne analogues were generated and examined in a Fourier transform ion cyclotron resonance mass spectrometer with the goal of comparing the reactivity and singlet–triplet gaps of the chlorinated and nonchlorinated benzyne. Theoretical calculations predict that the chloro isomers should have singlet–triplet gaps that differ by about 4 kcal/mol. Indeed, experiments confirm that the two singlet benzyne are separated in energy by 1.9 kcal/mol. Despite this difference, both isomers react at nearly identical rates that are as much as 2 orders of magnitude greater than the rates of the corresponding unchlorinated *m*-benzyne analogue. An interesting finding is that all of the *N*-phenylpyridinium *m*-benzyne ions react with *tert*-butyl isocyanide to form a strained, cyclic allene (although to different extents) that is almost 70 kcal/mol less stable than one of its hydrogen-shift isomers. The cyclic allene was characterized and quantified by collision-activated dissociation and ion–molecule reactions.

Introduction

The three isomeric didehydrobenzenes, the *o*-, *m*-, and *p*-benzynes, are important reactive intermediates and fundamentally interesting molecules. *o*-Benzyne (**1**) is by far the experimentally best characterized isomer in terms of both its structure and its reactivity. It has been isolated in a matrix¹ and probed with both IR² and UV–vis³ spectroscopy. In addition, *o*-benzyne intermediates are readily generated in solution from a variety of commercially available precursors and are known to react by concerted pericyclic pathways (e.g., Diels–Alder reactions).⁴



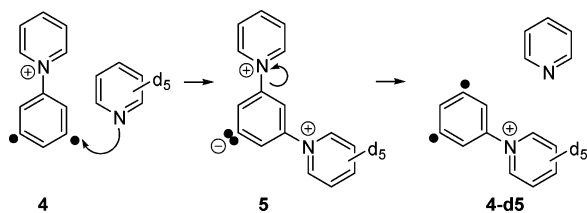
Recent interest in both *m*-benzyne (**2**) and *p*-benzyne (**3**) has stemmed largely from the discovery that *p*-benzyne intermediates are likely responsible for the antitumor activity of enediynes.⁵ Despite the importance of these intermediates, challenges in finding suitable precursors for the unambiguous generation of *m*- and *p*-benzynes, as well as the high reactivity of these species, has resulted in a paucity of experimental data regarding their structure and reactivity. Of the few condensed-phase experiments on the reactivity of *m*- and *p*-benzyne that do exist, many are inconclusive. For example, trapping experiments in solution have provided evidence for both the bicyclic⁶ (**2b** and **3b**) and biradical⁷ (**2** and **3**) structures of *m*- and *p*-benzyne. On the other hand, infrared spectroscopy of matrix-isolated *m*- and *p*-benzyne,⁸ in combination with a growing body of high-level calculations, support the diradicaloid structures **2** and **3**.⁹

Perhaps the key parameter that influences the structure, thermochemistry, and reactivity of the benzyne is the degree of interaction between the formally nonbonding orbitals containing the “biradical” electrons. A measure of this interaction is the singlet–triplet (ST) gap, which is defined as the energy difference between the singlet ground state and the lowest energy triplet state. An important step forward in the understanding of the chemistry of *o*-, *m*-, and *p*-benzynes was the utilization of negative ion photoelectron spectroscopy to measure accurately their ST gaps (-37.5 ± 0.3 , -21.0 ± 0.3 , and -3.8 ± 0.4 kcal/mol, respectively).¹⁰ Direct through-space interaction of the nonbonding orbitals in both **1** and **2** causes their relatively large ST gaps and low degree of biradical character (calculated¹¹ to be 11% and 20%, respectively) as well as their significantly distorted geometries. In contrast, **3** has only a small preference for a singlet ground state and hence enhanced biradical character¹¹ (65%) due to the weaker interactions of the nonbonding orbitals through the σ -bond framework of the molecule.¹²

Even though the ST gap of **3** is small, its effect on the molecule’s radical reactivity may be profound. It has been suggested^{13a} that the energetically favorable interaction between the biradical electron pair must be overcome for a radical reaction to occur, resulting in a larger reaction barrier and a decreased thermodynamic driving force relative to those of the same reaction for the analogous phenyl radical. However, this thinking was challenged^{13b} in a recent computational study that provides evidence for the involvement of the ground-state singlet and first excited singlet states, but not a triplet state, in the transition state of benzyne’s radical reactions. Nevertheless, solution experiments show that the hydrogen atom abstraction rates of *p*-benzyne, 1,4-didehydronaphthalene, and 9,10-didehydroanthracene are 1–2 orders of magnitude lower than those of the corresponding monoradicals.^{14,15} In addition, ab initio molecular orbital calculations predict that the barrier for hydrogen abstraction from methanol is about 1.5 kcal/mol larger for *p*-benzyne than for phenyl radical.^{13a} These observations have led to the suggestion that enediynes could be made more

* To whom correspondence should be addressed. E-mail: hilkka@purdue.edu.

SCHEME 1

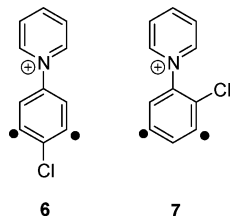


selective by increasing the ST gap of the biradical warhead (e.g., by adding appropriate substituents or by using a *m*-benzyne rather than a *p*-benzyne derivative).¹⁶

Indeed, there has been an increased effort to generate and study substituted benzyne. In a series of nice experiments, Sander and co-workers have used matrix-isolation techniques and spectroscopically characterized several substituted *m*-benzyne, including 2,4-didehydrophenol,^{17a} 3,5-didehydrofluorobenzene, 3,5-didehydrotoluene,^{17b} and tetrafluoro-3,5-didehydrobenzene.^{17c} Cramer and co-workers have systematically calculated the ST gaps of isomeric didehydropyridines and their protonated analogues,^{18a} didehydrophenols,^{18b} and didehydroanilines and benzonitriles.^{18c} However, there have been very few studies on the effect of substituents on the reactivity of *m*- or *p*-benzyne. One notable exception is the work of Chen et al., who examined the effect of protonation on the hydrogen atom abstraction reactions of 2,5-didehydropyridine.¹⁹

Some of the difficulties inherent to studies of reactive intermediates in condensed phases can be overcome by examining their reactivity in the low-pressure regime of a mass spectrometer. Gas-phase synthesis techniques have been developed to generate phenyl radicals and biradicals that bear an inert, charged substituent which allows for their mass spectrometric manipulation and study. Utilizing these techniques, the intrinsic reactivity of *o*-, *m*-,²⁰ and *p*-benzyne²¹ has been examined in a Fourier transform ion cyclotron resonance (FT-ICR) mass spectrometer.

Ion–molecule reactions of charged *m*-benzyne analogues have revealed a new type of electrophilic reactivity for this species (Scheme 1).²² This nucleophilic addition–elimination mechanism circumvents the need to uncouple the biradical electron pair and therefore explains many of the unexpectedly facile reactions of these charged *m*-benzyne. In this work, we report the synthesis of two isomeric chloro-substituted *m*-benzyne analogues, *N*-(4-chloro-3,5-didehydrophenyl)pyridinium (6) and *N*-(2-chloro-3,5-didehydrophenyl)pyridinium (7),

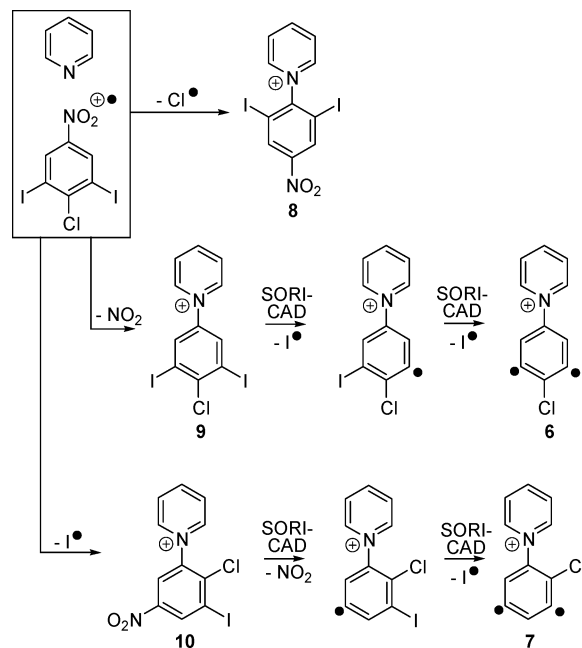


and compare their reactivity to that of the nonchlorinated *m*-benzyne analogue 4. Of particular interest is the influence of the electron-withdrawing chloro substituent on reaction rates, and its likely ability to stabilize charge-separated intermediates (e.g., 5). In addition, the chloro substituent should affect the relative stabilities of 6 and 7. This was examined experimentally via substitution reactions.

Experimental Section

All ion–molecule reactions were examined using a dual-cell Extrel model 2001 Fourier transform ion cyclotron resonance

SCHEME 2



mass spectrometer that has been described in detail elsewhere.²² The primary advantage of this instrument with respect to the study of complex ion–molecule reactions is that it contains a differentially pumped dual cell.²³ This design allows neutral precursors to be leaked into one side of the dual cell and ionized. Multiple ion isolation and reaction steps (MS^{*n*}) can be performed, if necessary, until the desired ion is synthesized. The ion of interest can then be selectively transferred into the second cell by grounding the middle plate common to both cells (conductance limit). In this way, the second cell can be used to conduct kinetic studies between an ion and a selected neutral reagent under conditions that are essentially free from contamination by neutral reagents that were necessary for generation of the ion.

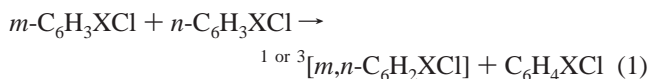
Charged *m*-benzyne analogues 6 and 7 were synthesized using a previously described technique that involves the formation of *N*-phenylpyridinium-type ions via an *ipso* substitution reaction between a pyridine nucleophile and a halobenzene radical cation.²⁴ In this case, both 6 and 7 can be synthesized by using the same halobenzene precursor, 4-chloro-3,5-diiodonitrobenzene. Electron ionization of 4-chloro-3,5-diiodonitrobenzene (typically 12–17 eV electron energy, 5 μ A beam current, and 50–100 ms beam time), followed by reaction with pyridine or 3-fluoropyridine (typical reaction times 4–6 s) resulted in abundant signals corresponding to *ipso* substitution occurring at the chloro, nitro, and iodo substituents (8–10, Scheme 2). *N*-Phenylpyridinium ions 9 and 10 are the precursors to 6 and 7, respectively. The desired *N*-phenylpyridinium precursor was selectively transferred into the other side of the dual cell by grounding the conductance limit for a short time (190–210 μ s). The technique of quadrupolar axialization was utilized to maximize transfer efficiency by refocusing the ions' cyclotron radius along the magnetic field axis prior to transfer.²⁵ After transfer into the other cell, the biradicals were synthesized by homolytically cleaving two carbon–iodo bonds in the case of 9 and a carbon–nitro bond followed by a carbon–iodo bond in the case of 10. Sequential bond cleavage was effected by using the technique of sustained off-resonance irradiated collision-activated dissociation (SORI-CAD; typically 1 kHz off-resonance for 200 ms) concurrent with a pulse of argon (maximum pressure in the cell $\sim 10^{-5}$ Torr).²⁶ After SORI-CAD,

a time delay of 1–2 s was used to allow the ions to release any excess translational and internal energy via collisions with neutral molecules and emission of IR photons. The biradicals were isolated by removing all other ions through the application of stored-waveform inverse Fourier transform (SWIFT) ejection pulses.²⁷

Kinetic data were obtained by allowing the isolated ions to react for variable periods of time with a neutral reagent present at a constant pressure prior to excitation and detection. A background correction was applied to ensure that the ionic products observed were formed from the desired ion population. Background spectra were generated by ejecting the reactant ions prior to the reaction time. Pseudo-first-order reaction rate constants were determined from the slope of a plot of the natural logarithm of the relative abundance of the reactant ion versus time. Second-order reaction rate constants (k_{rxn} , cm³ molecule⁻¹ s⁻¹) were obtained by dividing the pseudo-first-order rate constant by the absolute pressure (converted to molecules cm⁻³) of the neutral reagent. Corrections for the difference between the absolute pressure and the pressure measured by the ion gauges were obtained by measuring the rates for ion–molecule reactions assumed to proceed at the theoretical collision rate (e.g., exothermic electron-transfer reactions). Electron transfer to carbon disulfide radical cation was the reaction of choice to obtain correction factors for most of the neutral reagents in this work with the exception of ammonia and *tert*-butyl isocyanide. For these two reagents, a reaction involving exothermic proton transfer from protonated ethanol was utilized. Theoretical collision rates ($k_{\text{collision}}$) were calculated using a parametrized trajectory theory.²⁸ Reaction efficiencies used in this work are defined as $k_{\text{rxn}}/k_{\text{collision}} \times 100$ (i.e., the percent of collisions that are reactive).

4-Chloro-3,5-diiodonitrobenzene was synthesized by iodination of *p*-chloronitrobenzene via a procedure identical to that used for iodination of *p*-bromonitrobenzene.²⁹ The only deviation from the literature procedure was that the product was purified by recrystallization from methanol instead of ethanol. The elemental composition of the product was confirmed by measuring its exact mass, and its identity was confirmed by its fragmentation pattern upon 70 eV electron ionization. All other reagents were commercially available and were used as received.

Calculations. All geometries and energies reported in this work were calculated utilizing the Gaussian 98 suite of programs.³⁰ Geometry optimizations were carried out using density functional theory (DFT) with either the BLYP or BPW91 functional (vide infra). Each structure was verified to be a stationary point on the potential energy surface by analysis of vibrational frequencies at the same level of theory used to optimize the geometry. All reported energies include zero-point vibrational energy. The BLYP functional in conjunction with Dunning's correlation-consistent polarized valence double- ζ basis set (cc-pVDZ) was used in the calculation of the biradical stabilization energies (BSEs). The singlet and triplet BSEs were calculated using the same isodesmic reaction scheme employed previously by Cramer and co-workers for the study of substituted benzyne.¹⁸ First, the ΔH_{298} for the reaction in eq 1 was



calculated, where X = H in the case of the neutral molecules and X = pyridinium in the case of the charged molecules **6** and **7**. The enthalpy of this reaction is a measure of the stabilization or destabilization (relative to the monoradicals) that

results from placing both odd spins in the same ring. The BSEs calculated according to eq 1 were corrected for the difference between the BSEs calculated for *m*-benzyne by using eq 2



and its experimentally determined singlet and triplet BSEs (-20.6 ± 3.6 and 0.8 ± 2.8 kcal/mol, respectively).¹⁰ For 2,6-didehydrochlorobenzene and 2,4-didehydrochlorobenzene, BSEs were also calculated using the BD(T)/cc-pVDZ//BLYP/cc-pVDZ level of theory.

The 298 K ST gaps of the benzyne were obtained from the difference in their singlet and triplet BSEs. These values are reported in the text. The difference between the 298 and 0 K ST gaps was less than 0.3 kcal/mol. The ST gaps of the benzyne were also estimated using the hyperfine coupling constant method developed by Cramer and Squires.³¹ They found that there was a correlation between the ST gaps of benzyne, naphthalynes, and pyridynes calculated at the CASPT2/cc-pVDZ//CASSCF/cc-pVDZ level and the BPW91/cc-pVDZ-calculated isotropic hyperfine splitting (hfs) constant of the corresponding monoradical at the hydrogen atom that would have to be removed to generate the biradical of interest. For example, the hyperfine coupling constant at the 4-hydrogen in 2-dehydrochlorobenzene can be used to estimate the ST gap of 2,4-didehydrochlorobenzene. The relation between *ortho* and *meta* hfs's in monoradicals and the calculated ST gaps of the biradicals at the CASPT2/cc-pVDZ//CASSCF/cc-pVDZ level has been reported to be¹⁸

$$\text{ST gap (kcal/mol)} = [-1.39(^1\text{H hfs, G}) - 9.48] - 3.0 \quad (3)$$

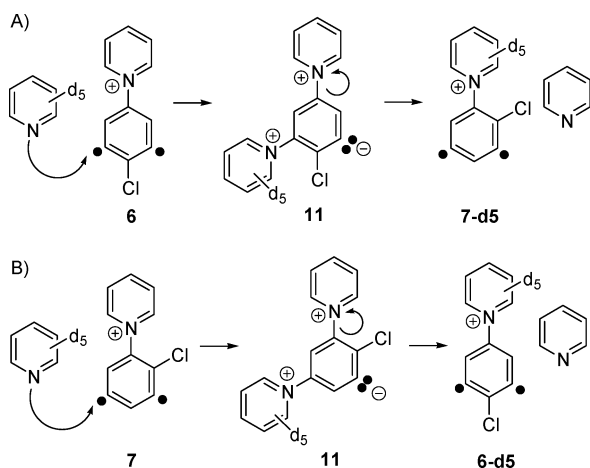
The correction of 3.0 kcal/mol is needed to correct for the difference in the CASPT2-calculated ST gap for *m*-benzyne (-18.0 kcal/mol) and its experimentally determined¹⁰ ST gap of -21.0 ± 0.3 kcal/mol. When this method was used, the geometries of the monoradicals were optimized and the hfs constants calculated using the BPW91/cc-pVDZ level of theory.

Results and Discussion

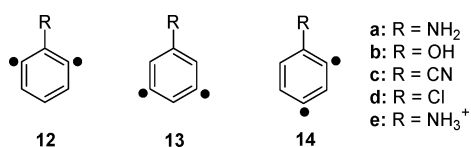
Ion Generation and Characterization. Chlorobenzyne isomers **6** and **7** were synthesized in the mass spectrometer according to previously published methods.²⁰ Briefly, electron ionization of 4-chloro-3,5-diiodonitrobenzene followed by subsequent reaction of the resulting radical cation with pyridine produces three major products corresponding to *ipso* substitution of the chloro, nitro, and iodo substituents of the radical cation (**8–10**, Scheme 2). Biradicals **6** and **7** are produced from **9** and **10** by isolating the appropriate precursor and homolytically cleaving two carbon–iodine bonds in **9** or a carbon–nitro bond followed by a carbon–iodine bond in **10**. Bond cleavage was effected by using SORI-CAD.²⁶

The structures of ions **6** and **7** can be verified and distinguished by examining their reactivity. Both **6** and **7** react with dimethyl disulfide by sequential abstraction of two thiomethyl groups, indicating the presence of two radical sites.²⁰ Isomerization to more stable *o*-benzyne isomers is ruled out since neither **6** nor **7** reacts with furan or thiophenol while the *o*-benzyne *N*-(3,4-didehydrophenyl)pyridinium forms addition products with these reagents.²⁰ Biradicals **6** and **7** can be interconverted via the charge-site substitution mechanism previously reported for *N*-phenylpyridinium analogues of *m*-benzyne (Schemes 1 and 3).²² The charge-site substitution products **6-d**₅ and **7-d**₅ in Scheme 3 and by analogy **6** and **7** can be distinguished on the basis of their reaction products with *tert*-

SCHEME 3



SCHEME 4



butyl isocyanide. Isomer **6** reacts with *tert*-butyl isocyanide by abstraction of cyanide and loss of chloride, while **7** reacts predominately by abstraction of hydrogen cyanide (*vide infra*). The reactions confirm that pyridine adds exclusively to the *m*-benzynes moiety and, in the case of the nonsymmetric isomer **7**, that pyridine adds regioselectively to the 5 position.

Isomer Thermochemistry. Johnson and Cramer have calculated the ST gaps of a variety of substituted *m*-benzynes (**12a–c**, **13a–c**, **14a–c**, Scheme 4) and rationalized the observed trends as a function of the inductive and conjugative properties of the substituent.^{18c} Briefly, σ -withdrawing and π -donating groups stabilize the singlet relative to the triplet state (i.e., the magnitude of the ST gap is larger) for the 2,6-isomers **12** (Scheme 4) and 3,5-isomers **13** (Scheme 4), although the effect is weaker in the latter case. For the 2,4-isomers **14** (Scheme 4), singlets are stabilized by σ -withdrawing and π -accepting substituents. The singlets are destabilized relative to the triplets (i.e., the magnitude of the ST is smaller) if the properties of the substituent are opposite those listed above. In the case of the π -donating amino substituent, the ST gap trend is **12a** > **13a** > **14a** with an almost 10 kcal/mol difference in the calculated ST gaps of **12a** and **14a**. The same trend is observed for hydroxy substitution although the calculated ST gap difference between **12b** and **14b** is about 2 kcal/mol less than for the corresponding amino isomers since the hydroxy substituent is a poorer π -donor.^{18b} In the case of the π -withdrawing cyano substituent, all three isomers have similar ST gaps (**12c** \approx **13c** \approx **14c**) calculated to be within about 1 kcal/mol of that of *m*-benzynes itself.

Since a chloro substituent is σ -withdrawing and very weakly π -donating, it is reasonable to assume that the ST gaps of *m*-didehydrochlorobenzynes **12d–14d** (Scheme 4) should follow the same trend as those of the *m*-didehydrophenols **12b–14b** although potentially somewhat muted. In addition, the chloro-substituted distonic *m*-benzynes **6** and **7** should have ST gaps similar to those of their neutral counterparts **12d** and **14d** on the basis of calculations^{18c} showing that the protonated amino group does not perturb the ST gap of 3,5-didehydroanilinium (**13e**; Scheme 4) relative to *m*-benzynes. To determine whether chloro substitution produces the anticipated ST gap effects, the

TABLE 1: Singlet and Triplet BSEs (kcal/mol, 298 K)^a of Various Benzynes

Benzynes	Theory	Singlet BSE	Triplet BSE
 12d	BLYP BD(T)	-24.5 -23.1	1.7 1.3
 14d	BLYP BD(T)	-19.7 -19.3	0.3 0.5
 6 : X = pyridinium	BLYP	-26.1	1.9
 7 : X = pyridinium	BLYP	-21.5	0.8
 4 : X = pyridinium	BLYP	-21.0	1.0
 2	Exp. ^b	-20.6 +/- 3.6	0.8 +/- 2.8

^a BLYP/cc-pVDZ-optimized geometries; see the text for the definition of BSEs. ^b Reference 10.

TABLE 2: ST Gaps (kcal/mol, 298 K)^a of Various Benzynes

Benzynes	Theory	ST gap
 12d	BLYP BD(T) hfc ^b	-26.2 -24.4 -23.8
 14d	BLYP BD(T) hfc ^b	-20.0 -19.8 -19.4
 6 : X = pyridinium	BLYP hfc ^b	-28.0 -24.2
 7 : X = pyridinium	BLYP hfc ^b	-22.3 -20.2
 4 : X = pyridinium	BLYP hfc ^b	-22.0 -20.9
 2	Exp. ^c	-21.0 +/- 0.3

^a BLYP/cc-pVDZ-optimized geometries unless indicated otherwise. ^b UBWP91/cc-pVDZ-optimized geometry; see the text for the definition of the method. ^c Reference 10.

singlet and triplet BSEs of **12d**, **14d**, **6**, **7**, and **4** were calculated (Table 1) via an isodesmic reaction scheme identical to that used in previous studies¹⁸ on substituted didehydrobenzenes and didehydronaphthalenes (see the Experimental Section). The BSEs were used to calculate the ST gaps of the chloro-substituted *m*-benzynes (Table 2). ST gap estimates were also made on the basis of a previously established correlation between the CASPT2/cc-pVDZ-calculated ST gaps of benzynes,

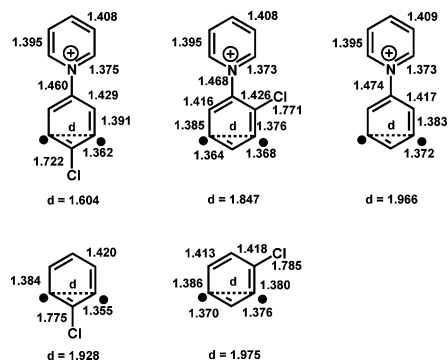


Figure 1. Heavy-atom bond lengths (Å) of singlet distonic *m*-benzyne ions and their neutral analogues as calculated at the BLYP/cc-pVDZ level of theory.

naphthalynes, and pyridynes and the BPW91/cc-pVDZ-calculated isotropic hfs constant at the hydrogen atom of the corresponding monoradical that would be removed to generate the biradical of interest (see the Experimental Section and Table 2).

As predicted, a chloro substituent between the radical sites stabilizes the singlet states of **12d** and **6** relative to *m*-benzyne by 3.9 and 5.5 kcal/mol, respectively (Table 1). In contrast, the isomeric “2,4-type” chlorobenzenes **14d** and **7**, as well as the unchlorinated *m*-benzyne distonic ion **4**, have singlet BSEs within 1 kcal/mol of the experimental value for *m*-benzyne. The triplet states are essentially unaffected by substitution as all triplet BSEs are within 1.1 kcal/mol of that of *m*-benzyne. The net result is that **12d** and **6** have larger ST gaps than their isomers **14d** and **7** by about 4–6 kcal/mol (Table 2). The size of **6** and **7** precludes the use of BD(T) for calculating their ST gaps, so only BLYP and hfc estimates are available. BLYP predicts an ST gap for **6** of -28.0 kcal/mol, which seems too large considering that the average CASPT2 and coupled-cluster values for the corresponding 2,6-didehydroaniline and 2,6-didehydrophenol are -28.3 and -27.0 kcal/mol, respectively.^{18b,c} Since the hfc method predicts ST gaps that are within 1 kcal/mol of the BD(T) calculations for **12d** and **14d**, it is likely that the hfc ST gap values of -24.2 and -20.2 kcal/mol are more appropriate estimates for **6** and **7**.

The geometries of the *m*-benzenes studied are shown in Figure 1 along with their unique heavy-atom bond lengths. Perhaps the only remarkable difference between the isomers is that BLYP/cc-pVDZ predicts a bicyclic structure for **6**. Pure DFT functionals have predicted bicyclic structures for other *m*-benzenes as well, including 3,5-didehydropyridine; however, higher level calculations at the CCSD(T) level predict essentially the same energy for the bicyclic and monocyclic structures.³² In fact, the bimolecular reactivity of **6** is more consistent with a monocyclic rather than a bicyclic structure (vide infra). The fact that BLYP appears to overestimate the bonding between the radical sites in **6** is likely the reason it predicts a ST gap for **6** that appears too large.

Isomers **6** and **7** can be interconverted through a common zwitterionic intermediate (**11**, Scheme 3) by substitution of the pyridine charge site with perdeuterated pyridine (Scheme 3). By measuring the rates of the “forward” (**7** to **6-d₅**, Scheme 3B) and “reverse” (**6** to **7-d₅**, Scheme 3A) charge-site substitution reactions, an equilibrium constant for a putative **7-d₅/6** equilibrium can be determined. On the basis of the calculated singlet BSEs, the forward reaction should be exothermic, and indeed, the charge-site substitution occurs with a moderate reaction efficiency ($k_{\text{reaction}}/k_{\text{collision}}$) of 14.5%. The endothermic reverse charge-site substitution reaction is considerably slower,

TABLE 3: Efficiencies^a and Products^b of the Reactions of Distonic *m*-Benzyne Ions with Selected Neutral Reagents

	7F	6F	4F
pyridine	substitution (100%) ^c eff = 25%	substitution (100%) ^c eff = 22%	substitution (100%) ^c eff = 2.0%
<i>t</i> -butyl isocyanide	HCN abs (90%) ^d 2° adduct CN abs (5%) 2° CN abs substitution (5%) ^c eff = 46%	CN - Cl (57%) 2° HCN abs HCN abs (43%) ^d 2° adduct eff = 42%	HCN abs (51%) ^d 2° adduct CN abs (33%) 2° CN abs substitution (14%) ^c adduct (2%) eff = 11%
dimethyl disulfide	SCH ₃ abs (100%) 2° SCH ₃ abs eff = 4.1%	SCH ₃ abs (100%) 2° SCH ₃ abs eff = 3.3%	SCH ₃ abs (100%) 2° SCH ₃ abs eff = 0.05%
allyl iodide	adduct (57%) I abs (43%) 2° I abs eff = 0.03%	Not done	No reaction
tetrahydrofuran	No reaction	No reaction	No reaction
thiophenol	No reaction	No reaction	No reaction
1,4-cyclohexadiene	No reaction	No reaction	No reaction
furan	No reaction	No reaction	No reaction

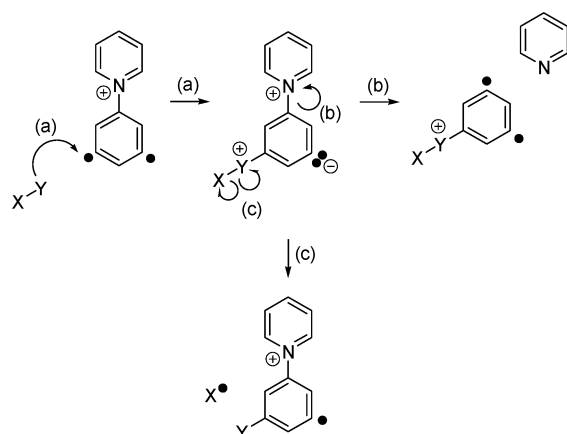
^a Reaction efficiencies (eff) reported as $k_{\text{exp}}/k_{\text{collision}} \times 100$. ^b Product branching ratios are given in parentheses. Secondary products (2°), if any were observed, are given underneath the primary product that produced them. ^c Substitution refers to addition of the neutral reagent followed by loss of the 3-fluoropyridine charge site. ^d The primary product corresponding to net HCN abstraction did not completely react away by adduct formation (see the text).

occurring with a reaction efficiency of 0.6%. These reaction rates yield an equilibrium constant of ~ 24 , which corresponds to a $\Delta\Delta G_{298}$ of ~ 1.9 kcal/mol. BLYP/cc-pVDZ calculations predict a ΔH_{298} difference between isomers **6** and **7** of 4.9 kcal/mol and a ΔG_{298} difference of 4.0 kcal/mol. This is consistent with the observation that BLYP appears to overstabilize singlet **6** relative to **7**. If one assumes that the hfc method provides a better estimate of the ST gaps of **6** and **7** ($\Delta(\text{ST gap}) = 4.0$ kcal/mol) and that ~ 1 kcal/mol of this difference is due to **6** having a ~ 1 kcal/mol larger triplet BSE than **7** (see Table 1), then one obtains a ΔH_{298} difference of ~ 3 kcal/mol (or a ΔG_{298} difference of ~ 2.1 kcal/mol, on the basis of the BLYP calculations). The small experimental $\Delta\Delta G_{298}$ of 1.9 kcal/mol is consistent with the fact that chlorine is a very poor π -donor and should only marginally stabilize the singlet **6** relative to **7**.

Reaction Efficiencies. Since the reactivity of the unchlorinated *N*-(3,5-didehydrophenyl)-3-fluoropyridinium ion (**4F**; Table 3) has been examined previously,²⁰ analogues of **6** and **7** were synthesized with a 3-fluoropyridine (**6F** and **7F**, Table 3) rather than a pyridine charge site to facilitate comparison between the systems. The effect of chlorine substitution on reaction rates is perhaps best illustrated by the reactions of the *m*-benzenes with pyridine and dimethyl disulfide. In the case of pyridine, all three *m*-benzenes react to yield a charge-site substitution product where pyridine replaces the weaker nucleophile 3-fluoropyridine; however, this charge-site substitution reaction occurs an order of magnitude faster for **6F** and **7F** (reaction efficiencies of 25% and 22%, respectively) than for **4F** (reaction efficiency of 2.0%). The situation is much the same with dimethyl disulfide, where **6F** and **7F** abstract a thiomethyl group with similar reaction efficiencies (4.1% and 3.3%, respectively) while **4F** reacts to yield the same product but at a significantly slower rate (efficiency of 0.05%).

Previous work²² has demonstrated that distonic *m*-benzyne analogues react to give net-radical products not via radical mechanisms but instead by nucleophilic addition pathways (Scheme 5) akin to the charge-site substitution reaction. The

SCHEME 5



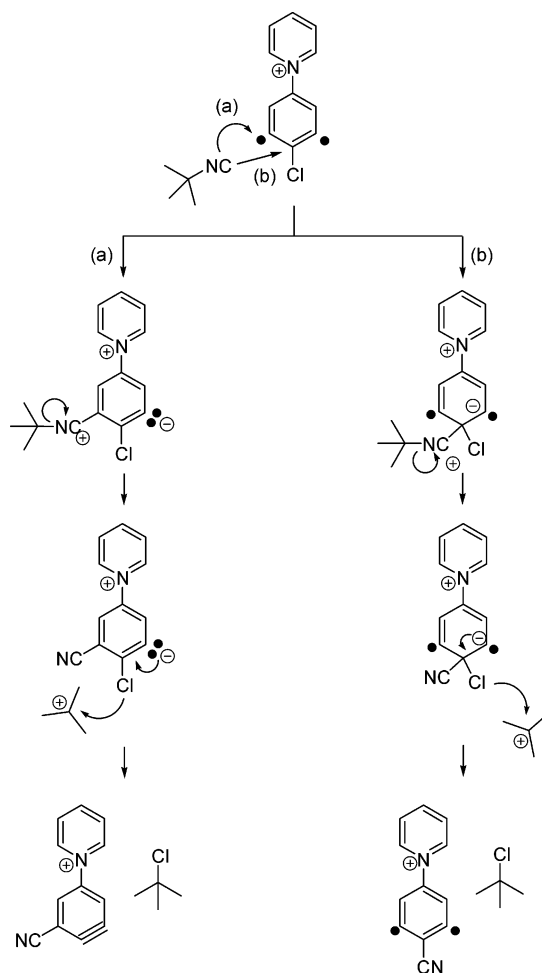
controlling factor between the formation of a charge-site substitution product and a net-radical abstraction product is the relative ability of the incoming nucleophile to replace the charge site (Scheme 5, path b) or to fragment (Scheme 5, path c) after addition to the benzyne moiety (Scheme 5, path a). For weak nucleophiles, such as dimethyl disulfide, substitution of a pyridine charge site is endothermic and only the fragmentation pathway is possible. For stronger nucleophiles that can fragment, such as *tert*-butyl isocyanide, both substitution and fragmentation pathways are feasible. Indeed, both charge-site substitution and net-radical products (e.g., CN abstraction) are observed in the reactions of **7F** and **4F** with *tert*-butyl isocyanide (Table 3).

If either the substitution or fragmentation pathway is exothermic, then the initial nucleophilic addition (Scheme 5, path a) is typically the rate-limiting step.²² The barrier to nucleophilic addition is due in part to an increase in charge separation. An electron-withdrawing substituent, such as chlorine in **6F** and **7F**, should increase the electron deficiency of the benzyne orbital, making it more susceptible to attack by nucleophiles. The increased electron deficiency of the chloro-substituted benzyne **7** and **6** is evident in their larger calculated adiabatic electron affinities of 5.7 and 5.5 eV compared to 5.2 eV for the unchlorinated benzyne **4**.³³ The calculated electron affinities follow the same trend as the reaction efficiencies, **7F** \approx **6F** $>$ **4F**, in the reactions of these ions with nucleophilic reagents. In addition, the chlorine substituent should also stabilize the developing negative charge in the addition intermediate. Indeed, pyridine addition to chlorobenzene **7** to form zwitterion **11** (Scheme 3B) is calculated to be ~ 4 kcal/mol more exothermic than pyridine addition to **4** to form **5** (Scheme 1). In general, these results indicate that the barrier for nucleophilic addition to *m*-benzyne is lowered by σ -electron-withdrawing substituents.

While nucleophilic addition to *m*-benzyne is enhanced by a chlorine substituent, hydrogen atom abstraction is not. Neither **6** nor **7** reacts with the hydrogen atom donor tetrahydrofuran, thiophenol, or 1,4-cyclohexadiene. That no radical abstraction is observed is not surprising and is in agreement with Chen's reactivity paradigm for singlet biradicals.¹⁶ The large ST gap of *m*-benzyne causes a proportionally large barrier for radical abstraction such that radical reactions are not energetically feasible in the gas phase.

Reaction Products with *tert*-Butyl Isocyanide. Insomuch as the reaction efficiencies with *tert*-butyl isocyanide follow the same pattern as the electron affinities, **7F** \approx **6F** $>$ **4F**, these reactions do not appear on the surface to be particularly interesting. A closer inspection of the unique products of these

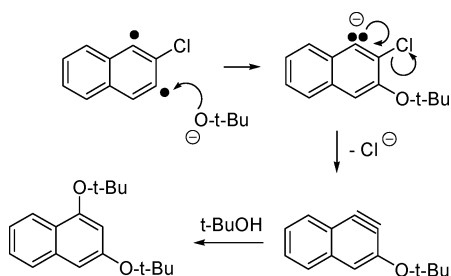
SCHEME 6



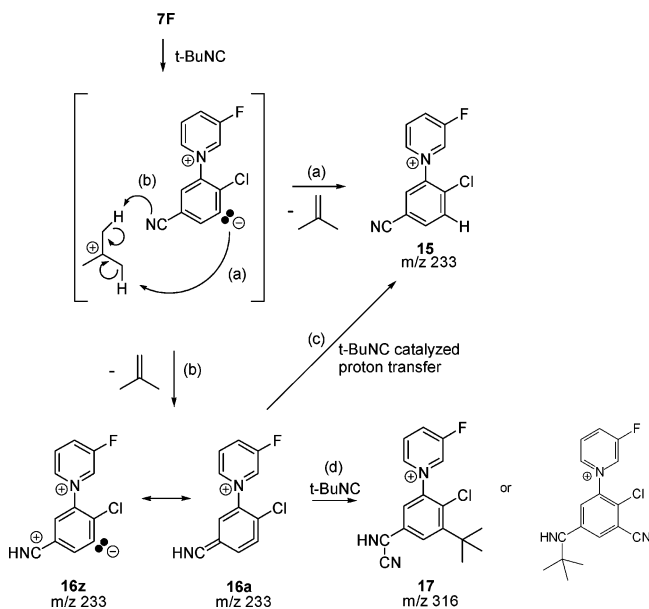
reactions, however, reveals more about the ionic reactivity of *m*-benzyne. For example, the major product in the reaction between *tert*-butyl isocyanide and **6F** corresponds to a net transfer of cyanide with an accompanying loss of chloride. The reaction could conceivably occur by addition of *tert*-butyl isocyanide to one of the dehydro carbons followed by fragmentation and loss of *tert*-butyl chloride to form an *o*-benzyne (Scheme 6, path a) or by addition of *tert*-butyl isocyanide to the *ipso* position relative to the chlorine substituent followed by fragmentation and loss of *tert*-butyl chloride to form a new substituted *m*-benzyne (Scheme 6, path b).

Calculations at the BLYP/6-31+G(d) level predict that formation of the cyano-substituted *o*-benzyne (Scheme 6, path a) is exothermic by 23 kcal/mol and formation of the cyano-substituted *m*-benzyne (Scheme 6, path b) is exothermic by 14 kcal/mol, suggesting that both pathways are feasible. However, the reactivity of the product corresponding to transfer of cyanide followed by loss of chloride is consistent with it possessing an *o*-benzyne structure. The isolated product reacts with *tert*-butyl isocyanide exclusively by HCN abstraction and with furan by addition and addition followed by loss of acetylene. Such reactivity is characteristic of *o*-benzyne but not *m*-benzyne.²⁰ The fact that addition occurs at the *m*-benzyne moiety has implications on the structure of the *m*-benzyne. As Kraka and co-workers point out, the LUMO of a bicyclic *m*-benzyne is a π^* orbital that should direct a nucleophile to the position *ipso* to the chlorine atom in **6F**, yielding a *m*-benzyne (Scheme 6, path b) rather than an *o*-benzyne.^{9a} Since the *m*-benzyne product is not observed, it is likely that **6F** possesses a "monocyclic" rather than bicyclic structure.

SCHEME 7



SCHEME 8



It is interesting to note that there is precedence for this type of reactivity. Billups et al. generated 2-chloro-1,3-didehydronaphthalene (Scheme 7) by sequential dehydrohalogenation of 1-bromo-3,4-benzo-6,6-dichlorobicyclo[3.1.0]hexane using *tert*-butoxide in tetrahydrofuran.^{7a} While they did observe a product corresponding to two hydrogen atom abstractions from tetrahydrofuran as 7% of their product yield, eight products accounting for 87% of the product yield can be accounted for by invoking addition of an anionic nucleophile (chloride, bromide, or *tert*-butoxide) to the *m*-benzyne moiety. One of these products, 1,3-di-*tert*-butoxynaphthalene, was proposed to arise by addition of *tert*-butoxide followed by loss of chloride to generate the *o*-benzyne 1-*tert*-butoxy-2,3-didehydronaphthalene (Scheme 7). Addition of *tert*-butyl alcohol to the *o*-benzyne results in the final observed product.

Chloro-substituted biradical **7F** also produces interesting reaction products. Reaction of **7F** with *tert*-butyl isocyanide results in the net abstraction of hydrogen cyanide as the major product (90% of the product branching ratio, Table 3), which may reasonably be anticipated to be *N*-(2-chloro-5-cyanophenyl)-3-fluoropyridinium (**15**; Scheme 8). However, a careful examination of secondary reaction products indicates that this intuitive assumption may be at least partially incorrect. A mass spectrum (Figure 2) taken after an intermediate reaction time between **7F** (*m/z* 206) and *tert*-butyl isocyanide (molecular weight 83) shows the formation of the primary HCN abstraction product (*m/z* 233) and an unexpected secondary reaction product of *m/z* 316. The following experimental observations regarding the *m/z* 233 and *m/z* 316 ion populations cast doubt on assigning structure **15** to the entire *m/z* 233 ion population.

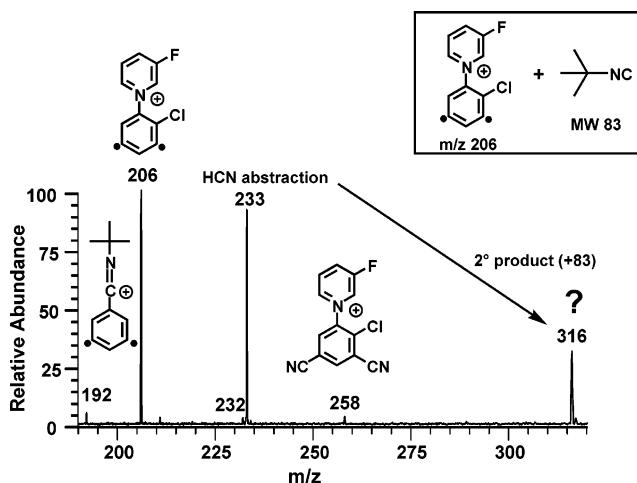


Figure 2. Mass spectrum corresponding to a 3.0 s reaction between **7F** and *tert*-butyl isocyanide.

First, continuous ejection of the *m/z* 233 ion population during a given reaction time (i.e., a double-resonance experiment) results in disappearance of the product of *m/z* 316. In addition, isolation of the *m/z* 233 ion population and subsequent reaction with *tert*-butyl isocyanide results in exclusive formation of *m/z* 316. These experiments confirm that the *m/z* 316 product arises from net addition of *tert*-butyl isocyanide to the HCN abstraction product of *m/z* 233. However, addition of *tert*-butyl isocyanide to the closed-shell structure **15** does not appear likely. Second, collision-activated dissociation (CAD) of the *m/z* 316 ion population results in loss of a methyl radical at low CAD energies and loss of a methyl radical and a chlorine atom at higher energies. This fragmentation suggests that the product of *m/z* 316 has a covalently bound structure and rules out a simple electrostatic adduct between **15** and *tert*-butyl isocyanide (as this adduct should dissociate by loss of *tert*-butyl isocyanide). Finally, the *m/z* 233 population does not completely react away. After long reaction times, the ratio of *m/z* 233 to *m/z* 316 becomes constant at $\sim 1.27:1$. This observation suggests that the *m/z* 233 ion population may consist of a mixture of isomers, one of which reacts with *tert*-butyl isocyanide to form the product of *m/z* 316 while the other is unreactive.

A reaction mechanism (Scheme 8) involving the formation of an HCN abstraction product with a strained cyclic allene structure (**16a**) can explain the above observations. *tert*-Butyl isocyanide can add to the benzylic carbon of **16a** (Scheme 8, path d) followed by fragmentation and addition of the *tert*-butyl group to the “phenide” moiety to produce **17**. The adduct **17** possesses three benzyl–methyl bonds, which would rationalize the facile loss of methyl radical indicated by the CAD spectrum of the *m/z* 316 ion population. In addition, the allene product **16a** could rearrange via a base-catalyzed proton shift (Scheme 8, path c) to form the “conventional” HCN abstraction product, which would explain the unreactive portion of the *m/z* 233 ion population. Calculations at the BLYP/6-31+G(d) level of theory predict that formation of cyclic allene **16a** is exothermic by almost 22 kcal/mol; however, the calculations also show that **16a** is 68 kcal/mol less stable than its more conventional isomer **15**. The calculated geometry of **16a** is more consistent with the strained cyclic allene structure than the zwitterionic one **16z** (vide infra).

Despite the fact that **16a** is significantly less stable than **15**, collision-activated dissociation experiments and ion–molecule reactions confirm that **16a** is indeed formed in the reaction of **7F** with *tert*-butyl isocyanide. After short reaction times, low-energy CAD of the isolated *m/z* 233 ion population results in

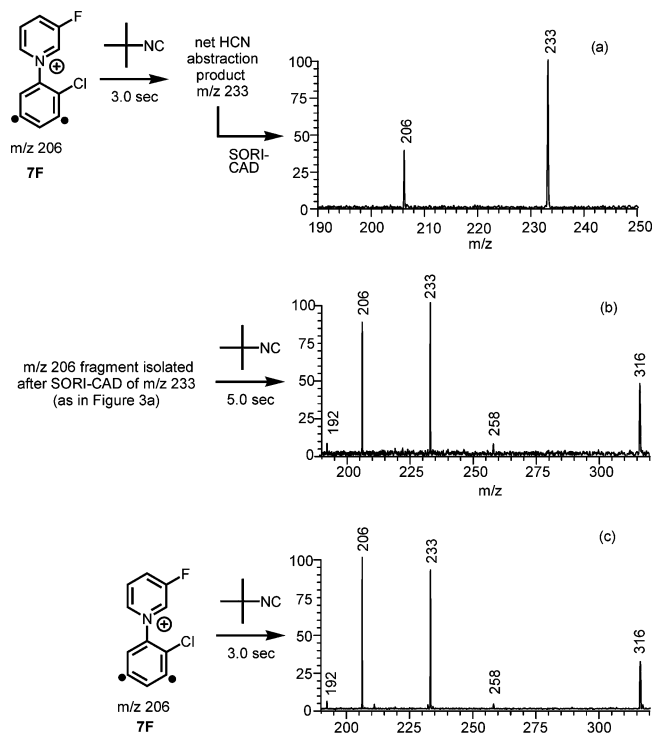


Figure 3. (a) Mass spectrum showing SORI-CAD of the isolated HCN abstraction product (m/z 233) after a 3.0 s reaction between **7F** and *tert*-butyl isocyanide. (b) Mass spectrum measured after a 3.0 s reaction between the isolated HNC loss product (m/z 206) formed from (a) and *tert*-butyl isocyanide. (c) Mass spectrum measured after a 5.0 s reaction of **7F** (m/z 206) with *tert*-butyl isocyanide. The identical spectra in (b) and (c) confirm that the CAD fragment m/z 206 in (a) has structure **7F**.

facile loss of hydrogen isocyanide to form an ion of m/z 206 (Figure 3a). Loss of hydrogen isocyanide from the allene **16a** should result in formation of biradical **7F**. Indeed, reaction of the fragment of m/z 206 (resulting from CAD of **16a**) with *tert*-butyl isocyanide (Figure 3b) results in a product distribution identical to that of independently generated **7F** (Figure 3c). After long reaction times, allene **16a** should have completely rearranged to lower energy isomer **15** (Scheme 8, path c) assuming that *tert*-butyl isocyanide is basic enough to remove the proton from the benzonitrile moiety in **16a**. Indeed, CAD of the remaining m/z 233 ion population after long reaction times results in loss of HCl and HF, while no HNC loss is observed (Figure 4a). The exact same fragmentation pattern is produced by CAD of authentic **15** (Figure 4b) generated by an *ipso* substitution reaction between 3-fluoropyridine and 4-chloro-3-nitrobenzotrile. As expected, the independently generated **15** is unreactive toward *tert*-butyl isocyanide.

A simple kinetic scheme (Scheme 9) based on the proposed mechanism (Scheme 8) provides a method for utilizing ion-molecule reactions to verify the existence of allene **16a** and to obtain at least semiquantitative information regarding the amounts of allene **16a** and its lower energy isomer **15** that are initially formed in the reaction of **7F** with *tert*-butyl isocyanide. The final ratio (i.e., the ratio at infinite reaction time) of the abundance of **15** (m/z 233) to the sum of the abundances of **15** and **17** (m/z 233 and m/z 316) is determined by the initial amounts of primary products **15** and **16a** and the partitioning of allene **16a** between rearrangement to form **15** (m/z 233) and adduct formation with *tert*-butyl isocyanide to form **17** (m/z 316). This partitioning is controlled by the relative rate constants for rearrangement by *tert*-butyl isocyanide (k_{r1} , Scheme 9) and

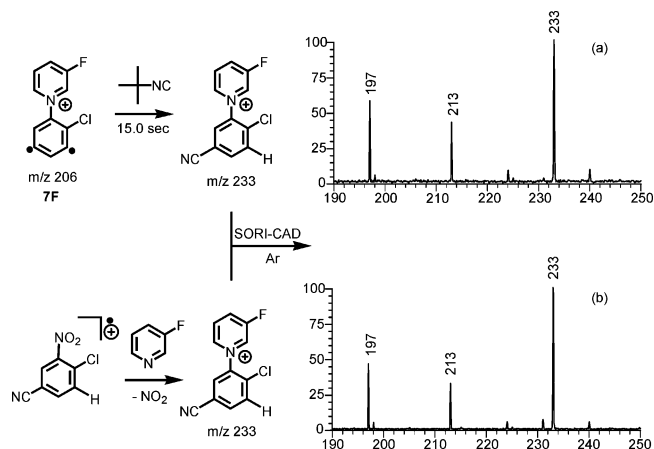
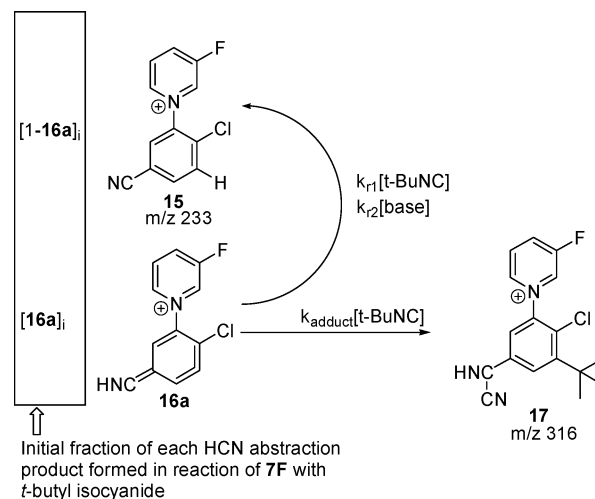


Figure 4. (a) SORI-CAD spectrum of the HCN abstraction product (m/z 233) measured after a 15 s reaction between **7F** and *tert*-butyl isocyanide. (b) SORI-CAD spectrum of authentic **15** (m/z 233).

SCHEME 9



$$\frac{15}{15 + 17} = \frac{[1-16a]_i + [16a]_i \frac{[P_{\text{normalized}}]}{[P_{\text{normalized}}] + (k_{\text{adduct}}/k_r)}}{[P_{\text{normalized}}] + (k_{\text{adduct}}/k_r)}$$

at time = ∞ if $k_{r1} = k_{r2} = k_r$

$$[P_{\text{normalized}}] = \frac{[t\text{-BuNC}] + [\text{Base}]}{[t\text{-BuNC}]}$$

adduct formation with *tert*-butyl isocyanide (k_{adduct} , Scheme 9). If a basic reagent is added that only reacts with the allene **16a** via the rearrangement pathway, then the rearrangement pathway is enhanced at the expense of adduct formation and the fraction of m/z 233 produced should increase as a function of the pressure of the basic reagent. If one makes the assumption that the rate constants for isomerization of allene **16a** caused by *tert*-butyl isocyanide (k_{r1}) and the added base (k_{r2}) are equal ($k_{r1} = k_{r2} = k_r$), then the initial amounts of **15** ($1 - [16a]_i$) and **16a** ($[16a]_i$) formed, as well as the ratio of rate constants k_{adduct}/k_r , can be found by fitting eq 4, where $P_{\text{normalized}} = (P_{t\text{BuNC}} + P_{\text{base}})/P_{t\text{BuNC}}$.

$$\frac{[m/z\ 233]}{[m/z\ 233] + [m/z\ 316]} = 1 - [16a]_i + [16a]_i \left(\frac{P_{\text{normalized}}}{P_{\text{normalized}} + (k_{\text{adduct}}/k_r)} \right) \quad (4)$$

The assumption that the added basic reagent only reacts by rearranging the allene **16a** is easily verified by observing that no additional products appear in the reaction spectrum. The

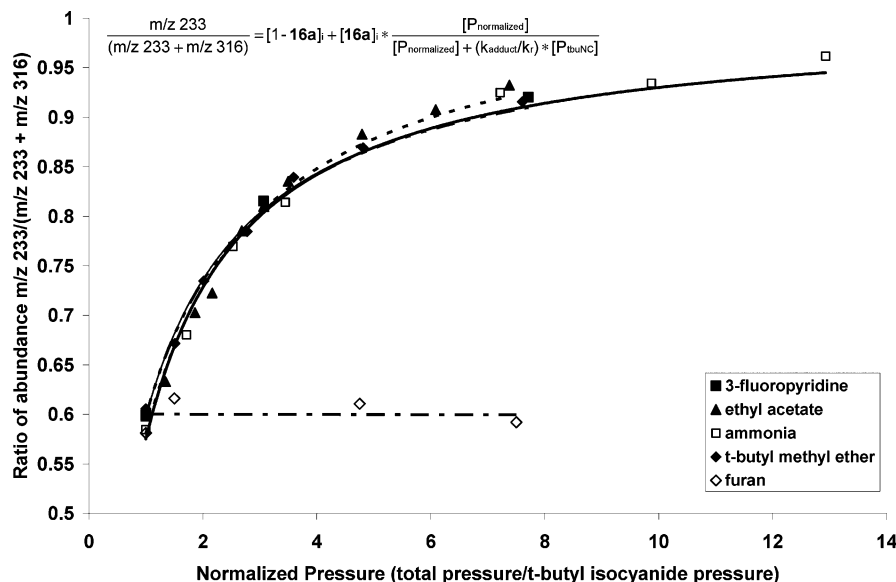


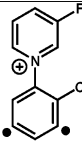
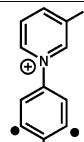
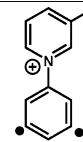
Figure 5. Final ratio $15/(15 + 17)$ (i.e., at long reaction times) for the reaction of **7F** with *tert*-butyl isocyanide at a constant pressure in the presence of a varied pressure of the indicated basic reagent. The best fit lines to eq 4 (see the text) for 3-fluoropyridine and *tert*-butyl methyl ether are obscured by the best fit line for ammonia (—). The best fit lines for ethyl acetate (---) (to eq 4) and furan (- · -) (to $y = mx + b$) are also shown.

assumption that the rearrangement rate constants k_{r1} and k_{r2} are equal is reasonable since any base capable of removing the proton from the benzonitrile group of **16a** should deposit the proton at the thermodynamically favored phenide moiety. If this assumption is valid, then the fraction of *m/z* 233 produced as a function of the pressure of the added base should be independent of the base used.

Indeed, the fraction of the ions of *m/z* 233 produced does increase when basic reagents are added (Figure 5), and the dependence of the ratio of the abundance of **15** to the sum of the abundances of **15** and **17** on the pressure of the added base is modeled well by eq 4. The nonlinear least-squares curve fits to eq 4 are shown in Figure 5 and are nearly identical for the bases 3-fluoropyridine, ammonia, and *tert*-butyl methyl ether (proton affinities (PAs) of 215.6, 204.0, and 201.1 kcal/mol,³⁴ respectively). Ethyl acetate (PA of 199.7 kcal/mol)³⁴ gives a similar curve; however, this experiment was complicated by the fact that a slow addition reaction occurred between ethyl acetate and allene **16a**. The best fit parameters to eq 4 for the nonlinear curves obtained via experiments in which the ratio of the abundance of **15** to the sum of the abundances of **15** and **17** was measured as a function of the pressure of a basic reagent (varied) in the presence of a constant pressure of *tert*-butyl isocyanide are shown in Table 4. In the case of **7F**, a majority (>80%) of the initial HCN abstraction product corresponds to the higher energy isomer **16a**. In contrast, reaction of *tert*-butyl isocyanide with both **6F** and **4F** produces much less (~25–30%) of **16a** relative to the conventional isomer **15**. For all of the biradicals, the curve fits indicate that the ratio of rate constants k_{adduct}/k_r is ~1.0, which is not surprising considering that both pathways should be considerably exothermic and both rate constants may be near the theoretical collision rate.

Figure 5 also shows that adding furan into the *tert*-butyl isocyanide reaction mixture does not enhance the isomerization pathway. The proton affinity at the benzonitrile nitrogen of the conjugate base of allene **16a** is calculated to be 211.9 kcal/mol (at BLYP/6-31+G(d) via an isodesmic reaction with protonated benzonitrile). The proton affinity of furan is 192.0 kcal/mol.³⁴ This suggests that proton transfer from allene **16a** to furan is endothermic by ~20 kcal/mol. A typical gas-phase ion–

TABLE 4: Best Fit Parameters to Eq 4 for Several Different Basic Reagents^a

Base	Fit parameters			
		7F	6F	4F
<i>t</i> -butyl methyl ether	[16a] ^b k_{adduct}/k_r ^c <i>r</i> ^{squared}	0.84 +/- 0.07 0.91 +/- 0.11 0.9949	0.24 +/- 0.02 0.98 +/- 0.12 0.9930	0.30 +/- 0.04 0.93 +/- 0.18 0.9769
ammonia	[16a] ^b k_{adduct}/k_r ^c <i>r</i> ^{squared}	0.97 +/- 0.15 0.77 +/- 0.18 0.9908	0.27 +/- 0.03 1.15 +/- 0.20 0.9902	
ethyl acetate	[16a] ^b k_{adduct}/k_r ^c <i>r</i> ^{squared}	0.88 +/- 0.08 1.04 +/- 0.14 0.9883		

^a See the text for eq 4 and a description of the isomerization experiment. The best fit curves are shown with the raw data in Figure 5. The errors shown are the standard errors of the nonlinear least-squares curve fit. ^b Fraction of HCN abstraction product that is initially allene **16a**. ^c Ratio of rate constants for adduct formation and rearrangement (see Scheme 9).

molecule collision complex does not release enough energy from solvation (~10–15 kcal/mol) to drive such an endothermic process.

Finally, some comments should be made regarding the structure and stability of the cyclic allene product arising from HCN abstraction by biradical **7F**. The BLYP/6-31+G(d)-optimized geometry of the pyridinium analogue of **16a** (**18a**, Figure 6) shows that the phenyl ring is significantly distorted from planarity as is characteristic of cyclic allenes.³⁵ The dihedral angles at the allene moiety are calculated to be -10.6° and -9.3° within the ring (C1–C2–C3–C4, C5–C4–C3–C2), while the dihedral angles including the attached substituents are 156.2° and 163.8° (C12–C2–C3–C4, H4–C4–C3–C2). The bond angle around the allene (C2–C3–C4) is 124.3° , which is larger than would be expected if C3 possessed a significant amount of phenyl anion character. For comparison, the analogous C–C–C bond angle in phenyl anion is 112.2° . It is worthy to note that the bispyridiniumphenide intermediates **5** (Scheme 1) and **11** (Scheme 3) exhibit some distortion from planarity as well, however not as dramatic as **18a**. The optimized geometry

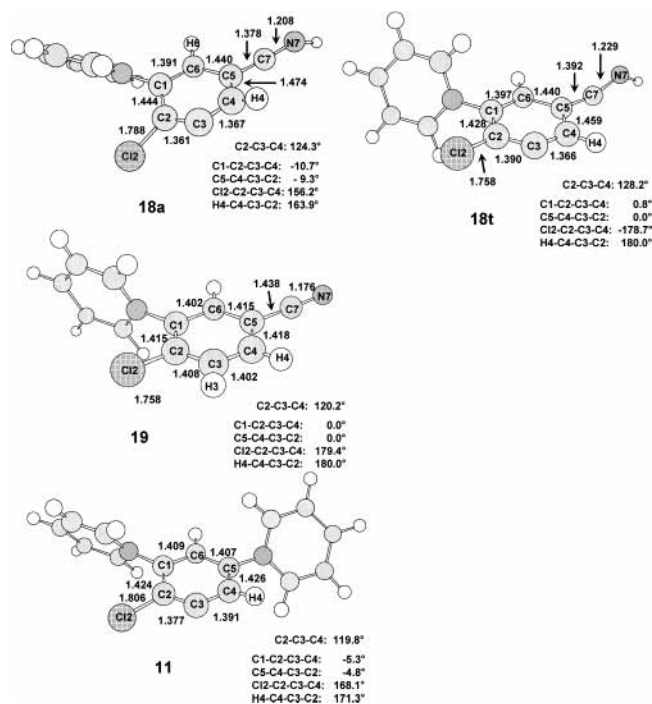


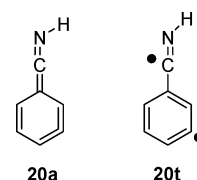
Figure 6. Heavy-atom bond lengths and selected angles and dihedral angles calculated at the BLYP/6-31+G(d) level of theory for the singlet and triplet states (**18a** and **18t**) of the allene product formed upon HCN abstraction by *N*-(2-chloro-3,5-didehydrophenyl)pyridinium from *tert*-butyl isocyanide, the conventional product arising from HCN abstraction for the same reaction (**19**), and the zwitterionic intermediate resulting from pyridine addition to *N*-(2-chloro-3,5-didehydrophenyl)pyridinium.

of **11** is shown in Figure 6. The dihedral angles at the phenide moiety are -5.3° and -4.8° within the ring (C1–C2–C3–C4, C5–C4–C3–C2) and 168.1° and 171.3° including the substituents (C12–C2–C3–C4, H4–C4–C3–C2). The bond angle around the allene (C2–C3–C4) is 119.8° , indicating increased electron density at C3 in **11** compared to **18a**.

Previously, the phenyl anion character of **5** was demonstrated in a flowing afterglow apparatus by its addition reaction with the strong electrophile boron trifluoride.^{22b} 2-Chloro-3,5-bispyridiniumphenide (**11**) is readily generated in the FT-ICR mass spectrometer as a product in the endothermic charge-site substitution reaction shown in Scheme 3a. Isolation of **11** and reaction with BF_3 resulted in an addition product even at low BF_3 pressures ($\sim 1.0 \times 10^{-8}$ Torr). In contrast, the addition of BF_3 ($\sim 10^{-7}$ Torr) into the reaction mixture of **7F** with *tert*-butyl isocyanide did not result in any BF_3 addition to allene **16a**. This finding is indicative of **16a** possessing decreased zwitterionic character and increased allene character relative to those of **11**.

The cyclic allene **18a** can also exist as an open-shell singlet or triplet biradical just like the analogous $\alpha,3$ -dehydrotoluene. The DFT calculations employed here place the allene 11.8 kcal/mol lower in energy than the corresponding triplet biradical (**18t**, Figure 6) and 68 kcal/mol higher in energy than the proton-shift isomer (**19**, Figure 6). As expected, the triplet **18t** has a planar geometry. These results are similar to published B3LYP/6-31++G(d,p) calculations on proton-shift isomers of benzonitrile.³⁶ In that work, the singlet allene (**20a**, Scheme 10) was calculated to be similar in energy to the triplet (**20t**, Scheme 10) and 88 kcal/mol higher in energy than benzonitrile itself. Given the size of **18a**, no attempt was made to calculate the energy of the open-shell singlet. However, the RDFT “wave function” of **18a** was stable with respect to breaking spin symmetry.

SCHEME 10



Conclusions

Gas-phase studies of reactive intermediates continue to provide experimental data that allow for the benchmarking of high-level theoretical calculations and for prediction of how such species may react in solution.³⁷ In this work, two chloro-substituted isomers of *m*-benzynes have been generated and the effect of the chloro-substituent on the reactivity and relative stability of the isomers has been investigated. In accord with previous predictions based on computational studies¹⁸ of substituted *m*-benzynes, *N*-(4-chloro-3,5-didehydrophenyl)pyridinium (**6**) was found via equilibrium measurements to be 1.9 kcal/mol more stable than the isomeric *N*-(2-chloro-3,5-didehydrophenyl)pyridinium (**7**).

In terms of their bimolecular reactivity, **6** and **7** react by electrophilic pathways, as reported previously for the nonchlorinated benzyne **4**. However, the chloro substituent serves to increase the electrophilicity of the *m*-benzyne moiety. Therefore, the rates of reaction of **6** and **7** with nucleophilic reagents are increased relative to that of **4** by as much as 2 orders of magnitude. The fact that **6** and **7** react at nearly identical rates despite the fact that **6** has a larger singlet–triplet gap by about 4 kcal/mol provides additional support for the earlier suggestion that *m*-benzynes react via ionic rather than radical mechanisms. Reaction of **6** with *tert*-butyl isocyanide resulted in formation of an *o*-benzyne by a mechanism similar to that proposed^{7a} over 20 years ago for the reaction of an analogous chloro-substituted *m*-benzyne in solution! Even more surprising was the discovery that the major product in the reaction of **7** with *tert*-butyl isocyanide is a cyclic allene that is 68 kcal/mol less stable than one of its proton-shift isomers. While it was beyond the scope of this work, further exploration of the bimolecular reactivity of this allene would be interesting as it may undergo cycloaddition reactions with dienes.

Acknowledgment. We thank the Jonathan Amy Facility for Chemical Instrumentation (JAFICI). Chris Petzold and Eric Nelson are acknowledged for many helpful and thought-provoking discussions. The NSF and the Lubrizol Corp. are thanked for providing funding for this research.

References and Notes

- (1) Chapman, O. L.; Mattes, K.; McIntosh, C. L.; Pacansky, J.; Calder, G. V.; Orr, G. *J. Am. Chem. Soc.* **1973**, *95*, 6134–6135.
- (2) Radziszewski, J. G.; Hess, B. A. J.; Zahradnik, R. *J. Am. Chem. Soc.* **1992**, *114*, 52–57.
- (3) Schweig, A.; Muenzel, N.; Meyer, H.; Heidenreich, A. *Struct. Chem.* **1990**, *1*, 89–100.
- (4) See for example: (a) Bowne, A. T.; Christopher, T. A.; Levin, R. H. *Tetrahedron Lett.* **1976**, *46*, 4111–4114. (b) Wittig, G. *Angew. Chem.* **1965**, *77*, 752–759. (c) Miller, R. G.; Stiles, M. *J. Am. Chem. Soc.* **1963**, *85*, 1798–1800. (d) Nunn, E. E. *Tetrahedron Lett.* **1976**, *46*, 4199–4202.
- (5) (a) Nicolau, K. C.; Dai, W.-M. *Angew. Chem., Int. Ed. Engl.* **1991**, *30*, 1387–1416. (b) Pratiel, G.; Bernadou, J.; Meunier, B. *Angew. Chem., Int. Ed. Engl.* **1995**, *34*, 746–769. (c) *Enediyne antibiotics as antitumor agents*; Borders, D. B., Doyle, T. W., Eds.; M. Dekker: New York, 1995; see also references therein.
- (6) For evidence of bicyclic structure **2b** see: (a) Washburn, W. N. *J. Am. Chem. Soc.* **1975**, *97*, 1615–1616. (b) Washburn, W. N.; Zahler, R. *J. Am. Chem. Soc.* **1976**, *98*, 7827–7830. For evidence of bicyclic structure

3b see: (c) Breslow, R.; Napierski, J.; Clarke, T. C. *J. Am. Chem. Soc.* **1975**, *97*, 6275–6276.

(7) For evidence of structure **2** see: (a) Billups, W. E.; Buynak, J. D.; Butler, D. *J. Org. Chem.* **1979**, *44*, 4218–4219. (b) Gaviña, F.; Luis, V. S.; Safont, V. S.; Ferrer, P.; Costero, A. M. *Tetrahedron Lett.* **1986**, *27*, 4779–4782. For evidence of structure **3** see: (c) Jones, R. R.; Bergman, R. G. *J. Am. Chem. Soc.* **1972**, *94*, 660–661.

(8) For a review see: Sander, W. *Acc. Chem. Res.* **1999**, *32*, 669–676.

(9) (a) Kraka, E.; Anglada, J.; Hjerpe, A.; Filatov, M.; Cremer, D. *Chem. Phys. Lett.* **2001**, *348*, 115–125. (b) Winkler, M.; Sander, W. *J. Phys. Chem. A* **2001**, *105*, 10422–10432.

(10) Wenthold, P. G.; Squires, R. R.; Lineberger, W. C. *J. Am. Chem. Soc.* **1998**, *120*, 5279–5290.

(11) Kraka, E.; Cremer, D. *Chem. Phys. Lett.* **1993**, *216*, 333–340.

(12) For descriptions of orbital interactions through bonds see: (a) Hoffman, R.; Imamura, A.; Hehre, W. J. *J. Am. Chem. Soc.* **1968**, *90*, 1499–1509. (b) Brunck, T. K.; Weinhold, F. *J. Am. Chem. Soc.* **1976**, *98*, 4392–4393. (c) Paddon-Row: M. N. *Acc. Chem. Res.* **1982**, *15*, 245–251.

(13) (a) Logan, C. F.; Chen, P. *J. Am. Chem. Soc.* **1996**, *118*, 2113–2114. However, see also: (b) Clark, A. E.; Davidson, E. R. *J. Am. Chem. Soc.* **2001**, *123*, 10691–10698.

(14) Roth, W. R.; Hopf, H.; Wasser, T.; Zimmermann, H.; Werner, C. *Liebigs Ann.* **1996**, 1691–1695.

(15) Schottelius, M. J.; Chen, P. *J. Am. Chem. Soc.* **1996**, *118*, 4896–4903.

(16) Chen, P. *Angew. Chem., Int. Ed. Engl.* **1996**, *35*, 1478–1480.

(17) (a) Bucher, G.; Sander, W.; Kraka, E.; Cremer, D. *Angew. Chem., Int. Ed. Engl.* **1992**, *31*, 1230–1233. (b) Sander, W.; Exner, M. *J. Chem. Soc., Perkin Trans. 2* **1999**, 2285–2290. (c) Wenk, H. H.; Sander, W. *Chem.—Eur. J.* **2001**, *7*, 1837–1844.

(18) (a) Debbert, S. L.; Cramer, C. J. *Int. J. Mass Spectrom.* **2000**, *201*, 1–15. (b) Johnson, W. T. G.; Cramer, C. J. *J. Am. Chem. Soc.* **2001**, *123*, 923–928. (c) Johnson, W. T. G.; Cramer, C. J. *J. Phys. Org. Chem.* **2001**, *14*, 597–603.

(19) Hoffner, J.; Schottelius, M. J.; Feichtinger, D.; Chen, P. *J. Am. Chem. Soc.* **1998**, *120*, 376–385.

(20) Thoen, K. K.; Kenttämaa, H. I. *J. Am. Chem. Soc.* **1999**, *121*, 800–805.

(21) Amegayibor, F. S.; Nash, J. J.; Lee, A. S.; Thoen, J.; Petzold, C. J.; Kenttämaa, H. I. *J. Am. Chem. Soc.* **2002**, *124*, 12066–12067.

(22) (a) Nelson, E. D.; Artau, A.; Price, J. M.; Kenttämaa, H. I. *J. Am. Chem. Soc.* **2000**, *122*, 8781–8782. (b) Nelson, E. D.; Artau, A.; Price, J. M.; Tichy, S. E.; Jing, L.; Kenttämaa, H. I. *J. Phys. Chem. A* **2001**, *105*, 10155–10168.

(23) Littlejohn, D. P.; Ghaderi, S. U.S. Patent 4,581,533, 1986.

(24) Thoen, K. K.; Kenttämaa, H. I. *J. Am. Chem. Soc.* **1997**, *119*, 3832–3833.

(25) Schweikhard, L.; Guan, S.; Marshall, A. G. *Int. J. Mass Spectrom. Ion Processes* **1992**, *120*, 71–83.

(26) Gauthier, J. W.; Trautman, T. R.; Jacobson, D. B. *Anal. Chim. Acta* **1991**, *246*, 211–245.

(27) Wang, T. C. L.; Ricca, T. L.; Marshall, A. G. *Anal. Chem.* **1986**, *58*, 2935–2938.

(28) (a) Su, T.; Chesnavich, W. J. *J. Chem. Phys.* **1982**, *76*, 5183–5185. (b) Chesnavich, W. J.; Su, T.; Bowers, M. T. *J. Chem. Phys.* **1980**, *72*, 2641–55.

(29) Tao, W.; Nesbitt, S.; Heck, R. *J. Org. Chem.* **1990**, *55*, 63–69.

(30) Frisch, M. J.; Trucks, G. W.; Schlegel, H. B.; Scuseria, G. E.; Robb, M. A.; Cheeseman, J. R.; Zakrzewski, V. G.; Montgomery, J. A., Jr.; Stratmann, R. E.; Burant, J. C.; Dapprich, S.; Millam, J. M.; Daniels, A. D.; Kudin, K. N.; Strain, M. C.; Farkas, O.; Tomasi, J.; Barone, V.; Cossi, M.; Cammi, R.; Mennucci, B.; Pomelli, C.; Adamo, C.; Clifford, S.; Ochterski, J.; Petersson, G. A.; Ayala, P. Y.; Cui, Q.; Morokuma, K.; Malick, D. K.; Rabuck, A. D.; Raghavachari, K.; Foresman, J. B.; Cioslowski, J.; Ortiz, J. V.; Stefanov, B. B.; Liu, G.; Liashenko, A.; Piskorz, P.; Komaromi, I.; Gomperts, R.; Martin, R. L.; Fox, D. J.; Keith, T.; Al-Laham, M. A.; Peng, C. Y.; Nanayakkara, A.; Gonzalez, C.; Challacombe, M.; Gill, P. M. W.; Johnson, B. G.; Chen, W.; Wong, M. W.; Andres, J. L.; Head-Gordon, M.; Replogle, E. S.; Pople, J. A. *Gaussian 98*, revision A.7; Gaussian, Inc.: Pittsburgh, PA, 1998.

(31) Cramer, C. J.; Squires, R. R. *J. Phys. Chem. A* **1997**, *101*, 9191–9194.

(32) Cramer, C. J.; Debbert, S. *Chem. Phys. Lett.* **1998**, *287*, 320–326.

(33) Calculated at (U)BLYP/6-31+G(d) on the corresponding anilinium rather than pyridinium benzyne.

(34) Hunter, E. P.; Lias, S. G. Proton Affinity Evaluation. In *NIST Chemistry WebBook*; Linstrom, P. J., Mallard, W. G., Eds.; NIST Standard Reference Database Number 69; National Institute of Standards and Technology: Gaithersburg, MD, July 2001 (<http://webbook.nist.gov>).

(35) Johnson, R. P. *Chem. Rev.* **1989**, *89*, 1111–1124.

(36) Flammang, R.; Barbieux-Flammang, M.; Gualano, E.; Gerbaux, P.; Le, H. T.; Nguyen, M. T.; Turecek, F.; Vivekananda, S. *J. Phys. Chem. A* **2001**, *105*, 8579–8587.

(37) For example for carbenes, see: (a) Schwartz, R. L.; Davico, G. E.; Radmond, T. M.; Lineberger, W. C. *J. Phys. Chem. A* **1999**, *103*, 8213–8221. (b) Seburg, R. A.; Hill, B. T.; Squires, R. R. *J. Chem. Soc., Perkin Trans. 2* **1999**, 2249–2256. (c) Clifford, E. P.; Wenthold, P. G.; Lineberger, C. W.; Petersson, G. A.; Broadus, K. M.; Kass, S. R.; Kato, S.; DePuy, C. H.; Bierbaum, V. M.; Ellison, G. B. *J. Phys. Chem. A* **1998**, *102*, 7100–7112. (d) Poutsma, J. C.; Paulino, J. A.; Squires, R. R. *J. Phys. Chem. A* **1997**, *101*, 5327–5336. For carbynes see: Jesinger, R. A.; Squires, R. R. *Int. J. Mass Spectrom.* **1999**, *185/186/187*, 745–757. For α,n -dehydrotoluenes see: Wenthold, P. G.; Wierschke, S. G.; Nash, J. J.; Squires, R. R. *J. Am. Chem. Soc.* **1994**, *116*, 7378–7392. For trimethylenemethane see: Wenthold, P. G.; Hu, J.; Squires, R. R.; Lineberger, W. C. *J. Am. Chem. Soc.* **1996**, *118*, 475–476.